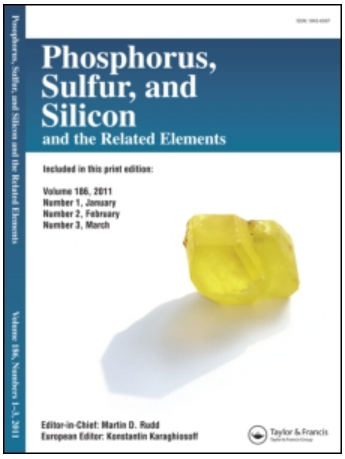

Phosphorus, Sulfur, and Silicon and the Related Elements
Publication details, including instructions for authors and subscription information:
http://www.informaworld.com/smpp/title~content=t713618290

PREPARATION AND NMR STUDY OF PHOSPHORUS-FLUORINE COMPOUNDS UNDERGOING INTRAMOLECULAR EXCHANGE. PART 3.[1] SUBSTITUTED FLUORODIAZADIPHOSPHETIDINES

Robin K. Harris[a]; Mohamed I. M. Wazeer[ab]; Ottfried Schlak[c]; Reinhard Schmutzler[c]
[a] School of Chemical Sciences, University of East Anglia, Norwich, England [b] Department of Chemistry, Peradeniya University, Sri Lanka [c] Lehrstuhl B für Anorganische Chemie der Technischen Universität, Pockelsstrasse, Germany

To cite this Article Harris, Robin K. , Wazeer, Mohamed I. M. , Schlak, Ottfried and Schmutzler, Reinhard(1981) 'PREPARATION AND NMR STUDY OF PHOSPHORUS-FLUORINE COMPOUNDS UNDERGOING INTRAMOLECULAR EXCHANGE. PART 3.[1] SUBSTITUTED FLUORODIAZADIPHOSPHETIDINES', Phosphorus, Sulfur, and Silicon and the Related Elements, 11: 2, 221 — 239
To link to this Article: DOI: 10.1080/03086648108077419
URL: http://dx.doi.org/10.1080/03086648108077419

Phosphorus and Sulfur, 1981, Vol. 11, pp. 221–239
0308-664X/81/1102-0221/$06.50/0

PREPARATION AND NMR STUDY OF PHOSPHORUS-FLUORINE COMPOUNDS UNDERGOING INTRAMOLECULAR EXCHANGE. PART 3.[1] SUBSTITUTED FLUORODIAZADIPHOSPHETIDINES.

ROBIN K. HARRIS and MOHAMED I. M. WAZEER†

School of Chemical Sciences, University of East Anglia, Norwich NR4 7TJ, England

and

OTTFRIED SCHLAK and REINHARD SCHMUTZLER

Lehrstuhl B für Anorganische Chemie der Technischen Universität, 33 Braunschweig, Pockelsstrasse 4, Germany

(*Received January 22, 1981*)

Proton, ^{19}F and ^{31}P NMR studies of a number of tetra-, tri- and di-fluorodiazadiphosphetidines have yielded information about the barriers to pseudorotation at the phosphorus atoms. The data are classified according to the process studied, and are discussed in terms of the feasible exchange mechanisms. The $\rangle PFR_2$ group is substantially more rigid than the $\rangle PF_2R$ group.

INTRODUCTION

The planar four-membered ring structure $\overline{P—N—P—N}$ for the diazadiphosphetidines has been confirmed for $[F_3PNMe]_2$ in the gas phase by electron diffraction[2] and for $[Cl_3PNMe]_2$, $[PhF_2PNMe]_2$, $[Ph_2FPNMe]_2$, $[(C_6F_5)F_2PNMe]_2$ and $[(Cl_3C)F_2PNMe]_2$ in the solid state by X-ray diffraction.[3–8] Diazadiphosphetidines are of particular interest because they contain two five-coordinate phosphorus atoms in a four-membered ring. It has been suggested[9] that pseudorotation at these phosphorus atoms can occur in a more-or-less concerted fashion. In order to obtain further insight into the mechanisms of pseudorotation in these diazadiphosphetidine systems, it was decided to study the barriers to pseudorotation in the compounds I–III (some additional compounds of type I were also examined).

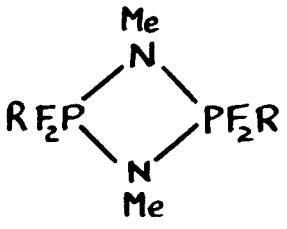

I

R = Me, Et, Pr^i, Bu^t, Ph
a b c d e

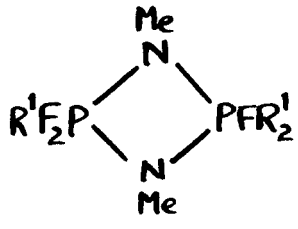

II

R^1 = Me, OMe
a b

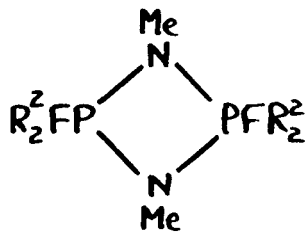

III

R^2 = Me, OMe
a b

† Present address: Department of Chemistry, Peradeniya University, Sri Lanka.

The most fruitful method of studying the geometry and intramolecular motion has proved to be NMR spectroscopy.[10,11] The preparations and the NMR parameters (^{19}F, ^{31}P and some ^{1}H) of the above comounds have been reported elsewhere.[10-14]

METHODS AND RESULTS

Fluorine-19 spectra of the tetrafluorodiazadiphosphetidines (I)

For compounds of the type I, the existence of *gauche* (IV) and *trans* (V) isomers has been demonstrated[10] by ^{19}F NMR studies at low temperatures. In each case the higher ^{19}F Larmor frequency has been assigned to the *gauche* isomer. However,

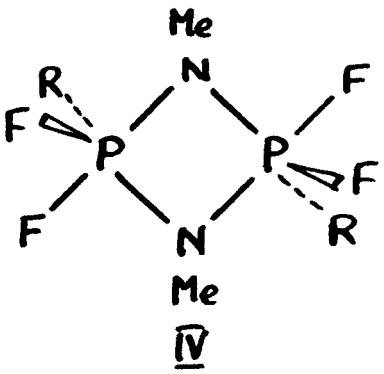

IV

gauche isomer

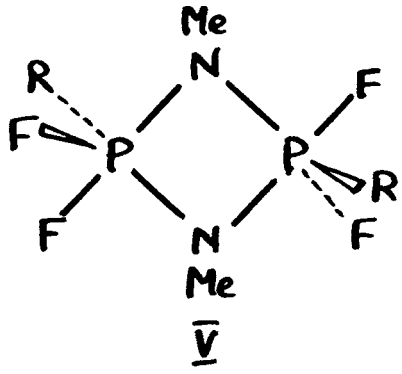

V

trans isomer

intramolecular exchange between the axial and equatorial fluorines is rapid on the NMR timescale and they are chemically equivalent even at the lowest temperatures used. The *gauche* $\rightleftharpoons$ *trans* exchange is a slower process and may be represented in NMR terms as:

$$[A[X]_2]_2 \rightleftharpoons [B[V]_2]_2$$

The exchanging spin systems are complex, and detailed bandshape analysis is difficult at present. However, in the ^{19}F spectra these symmetrical spin systems give sharp doublets, separated by $N_{AX} = |J_{AX} + J'_{AX}|$, which carry one-half of the intensity of the spectrum.[14] Thus it is possible, as an approximation, to consider only these "N lines" for exchange studies. Since $|N_{PF}|$ is very large (of the order of 950 Hz) in these samples the two halves of the N doublets can be considered independently (subspectra), to give two uncoupled two-site exchange cases with unequal populations (Figure 1).

At slow- and fast-exchange limits the bandshape of the N lines are slightly distorted by the $\chi = 2$ lines.[14] However, these lines are usually found only on one side of the N lines and the bandshape of the other side is unaffected. In the intermediate exchange region the distortion is very small.

Populations at low temperatures were determined by integration of the ^{19}F spectra (using the average of three integrals at each temperature). This was caried out for a range of temperatures below the slow-exchange limit. The high-temperature populations were obtained by extrapolation from a plot of ln K vs. 1/T (using the low temperature results) where K = [*gauche*]/[*trans*]. The values of $\Delta G^{\ominus}$ at 273 K, calculated from the extrapolated data for K, are given in Table 1. We do not believe the data are accurate enough to quote meaningful values of $\Delta H^{\ominus}$ and $\Delta S^{\ominus}$.

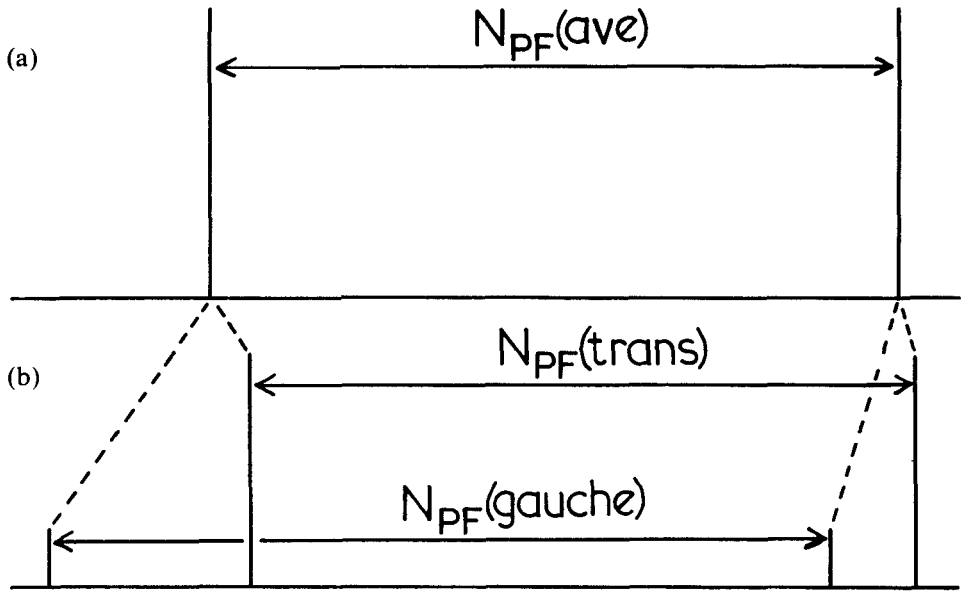

FIGURE 1 The variation with temperature of the "N doublet" lines in the ^{19}F spectra (diagrammatic) of compounds of the type $[RF_2PNMe]_2$: (a) high temperature; (b) low temperature. The thermodynamic parameters for the exchange were obtained from the intermediate bandshapes.

The ^{19}F bandshapes were partially simulated as described above using the Hahn, Maxwell[15] and McConnell[16] (HMM) equation. The population obtained for a particular temperature was kept constant in simulating the bandshape at that temperature. The value of T_2^* was obtained from the linewidth of the spectrum in the slow-exchange limit. The subspectral chemical shift difference between the two sites was found to be independent of the temperature in the slow-exchange region, and therefore was kept constant in the calculations. However, the average chemical shift was found to vary with temperature. The mean lifetime of the two isomers was varied

TABLE 1

Thermodynamic parameters[a] for $[RF_2PNMe]_2$ *trans*⇌*gauche* exchange

R	$\Delta H^{\ddagger}$/ kcal mol^{-1} (kJ mol^{-1})	$\Delta S^{\ddagger}$/ cal mol^{-1} deg^{-1} (J mol^{-1} K^{-1})	$\Delta G^{\ddagger}_{273}$/ kcal mol^{-1} (kJ mol^{-1})	$\Delta G^{\ominus\,\circ}_{273}$/ cal mol^{-1} (kJ mol^{-1})	T_c/°C
Me	9.7	−9.3	12.2	40	~0
	(40)	(−39)	(51)	(.2)	
Et	11.8	−4.6	13.1	260	~0
	(49)	(−19)	(55)	(1.1)	
Pr^i	15.1	−4.0	16.2[c]	580	~67[c]
	(63)	(−16)	(68)	(2.40)	
Bu^t	21.3	6.0	19.7[d]	870	~100[d]
	(89)	(25)	(82)	(3.6)	
Ph	8.1	−18.3	13.1	270	~0
	(34)	(−76)	(55)	(1.1)	

[a] Activation parameters are for the conversion of *trans* → *gauche*. A transmission coefficient $\kappa = 1$ has been used.

[b] Calculated from the equilibrium constant data.

[c] $\Delta G^{\ddagger}(T_c) = 16.5$ kcal mol^{-1} (69 kJ mol^{-1}).

[d] $\Delta G^{\ddagger}(T_c) = 19.1$ kcal mol^{-1} (80 kJ mol^{-1}).

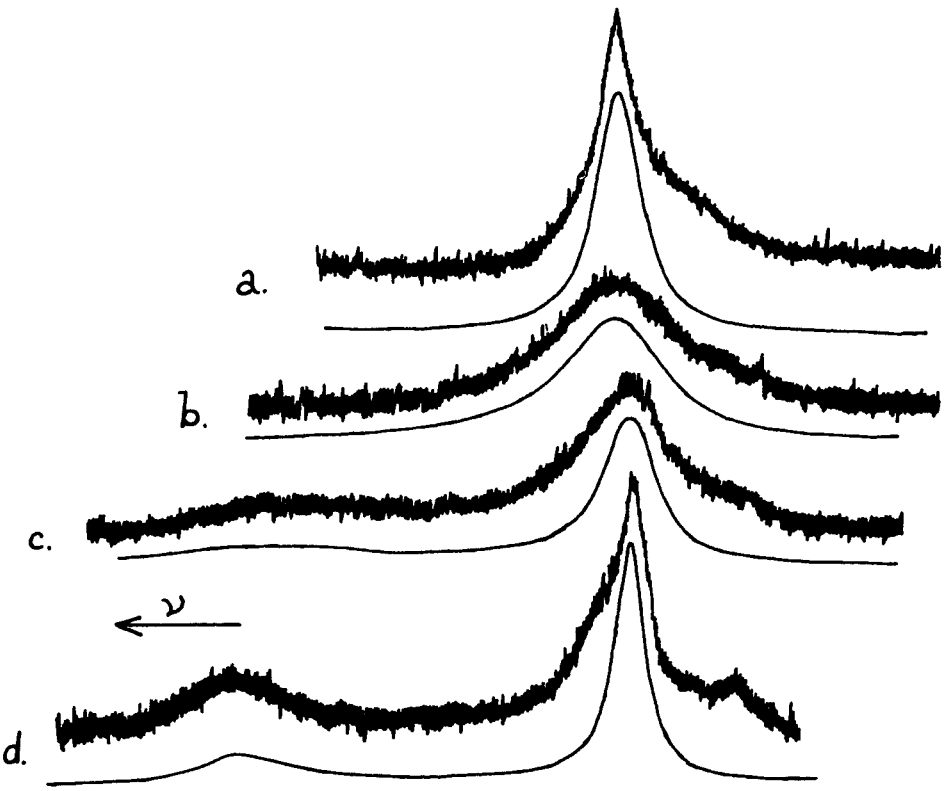

FIGURE 2 ^{19}F-{^{1}H} experimental and computer-simulated ^{19}F spectra (low-frequency moiety) for $[Pr^{i}F_2PNMe]_2$, as a function of temperature. The simulated spectra were obtained by consideration of the "N doublet" lines only. (a) 101°C, $k_t = 1388\ s^{-1}$; (b) 81°C, $k_t = 385\ s^{-1}$; (c) 61°C, $k_t = 119\ s^{-1}$; (d) 51°C, $k_t = 62\ s^{-1}$.

until a good fit of the calculated with the experimental spectrum was obtained. The fitting procedure was by eye (superposing the calculated on the experimental spectra). Some of the experimental and calculated spectra for Ic are shown in Figure 2. The majority of the calculations were carried out on the low-frequency subspectra. In some cases (Ia and Id) rate constants were also determined from high-frequency subspectra.

The rate constants k_t and k_g as given in:

$$trans \underset{k_g}{\overset{k_t}{\rightleftharpoons}} gauche$$

were obtained from the experimental mean rate constant by the relation $k_t = k_{obs.}P_g$ and $k_g = k_{obs.}P_t$, where P_t and P_g are the mole fractions of *trans* and *gauche* isomers respectively.

The values of k_t and k_g thus obtained were used with the Eyring equation to calculate the thermodynamic activation parameters. A plot of ln (k_t/T) against $1/T$ for Ic is given in the Figure 3. As a check $\Delta G\ddagger$ (*gauche*) values were also calculated using plots of ln (k_g/T) against $1/T$. The results of the calculations are given in Table I.

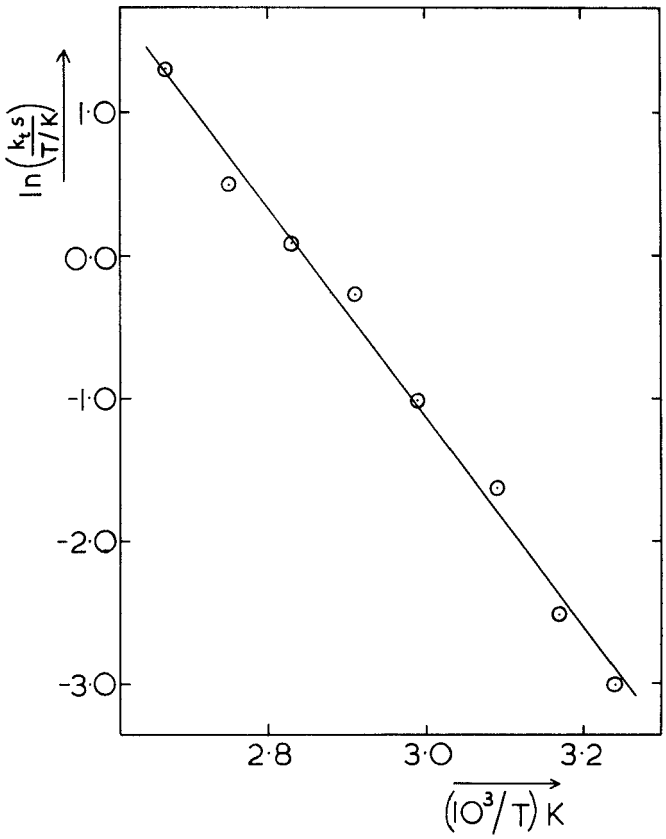

FIGURE 3 Eyring plot corresponding to the spectra of Figure 2, plus additional data.

Phosphorus-31 and fluorine-19 spectra of the trifluororodiazadiphosphetidines (II)

It has been shown that the axial⇌equatorial exchange of the fluorine atoms in the $>PF_2R^1$ group, can be slowed down on the NMR timescale for compounds of the type II. Such an exchange can be indicated by ABXYZ⇌ABYXZ. Once again complex spin systems are involved, and total bandshape analysis is not trivial. However, the $^{31}P-\{^1H\}$ spectrum for IIa is partially first order, and can be used for bandshape analysis. The central region for the $>PF_2Me$ group is shown in Figure 4. At high temperatures the two fluorines are magnetically equivalent but at low temperature they become anisochronous as the axial/equatorial exchange is slowed. The quartet structure is due to coupling to the distant phosphorus and fluorine nuclei. The exchange can be considered as four two-site processes with identical exchange rates and equal populations. The bandshapes were simulated using a computer program (WAX) specially written for this purpose, involving the HMM equation.[15,16] Unfortunately, the signal-to-noise ratio in the $^{31}P-\{^1H\}$ spectra was not good, especially in the intermediate exchange region. The spectra were recorded over a temperature range of 80°C. Calculated bandshapes were compared with the experimental ones by eye. The rate constant and temperature data were used in Eyring plots to obtain the activation parameters. The results obtained are given in the Table II.

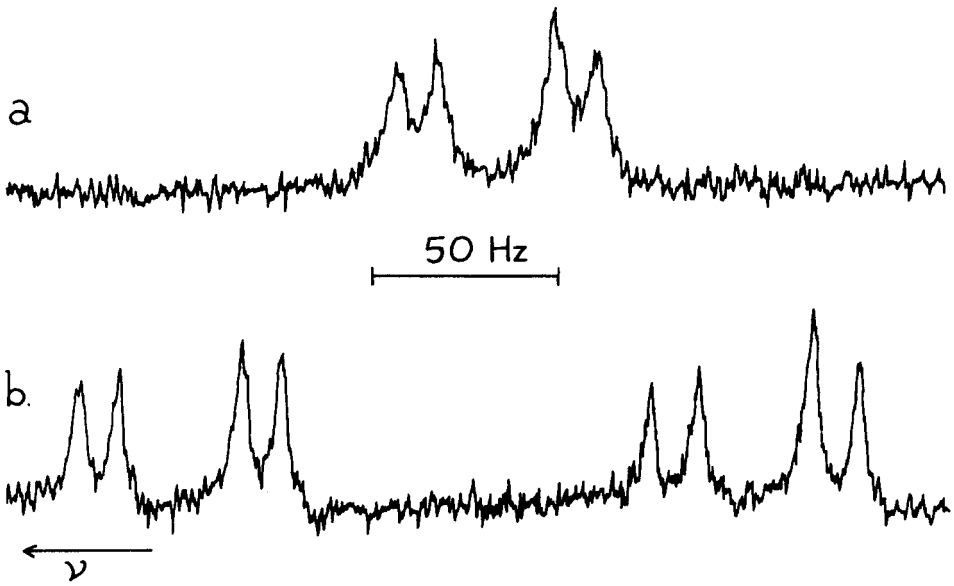

FIGURE 4 ^{31}P-{^{1}H} spectra (PF_2 central region only) for compound IIa: (a) +20°C; (b) ca. −60°C.

A similar bandshape analysis was not possible for IIb as the ^{31}P region is highly second order. An estimation of the barrier can be obtained from the coalescence temperature for the axial and equatorial fluorine resonances. The coalescence region is rather broad as the two coalescing signals are about 1500 Hz apart, but T_c was estimated to be -85 ± 10°C. The value of $\Delta G\ddagger_{188}$ is given in Table II.

Proton spectra of the trifluorodiazadiphosphetidines (II)

The room-temperature ^{1}H spectrum of IIa is first order, and shows a single environment for the $PFMe_2$ protons, together with a single value of $^{3}J_{FH}$ for the PF_2Me protons. This is consistent with rapid P—F bond equilibration, as expected from the ^{19}F and ^{31}P results. However, the protons of the two NMe groups are non-equivalent, and each couples differently to the two phosphorus nuclei. These facts show that P—N bond equilibration is slow on the NMR timescale. This situation remains up to at least 80°C (for a solution in ortho-dichlorobenzene), at which temperature there is still no sign of exchange broadening. At low temperature (−60°C) the spectrum becomes more complex (while remaining first order) since the $PFMe_2$ methyl groups become non-equivalent (as axial$\rightleftharpoons$equatorial exchange of fluorines in the PF_2Me group is slowed). In addition, the Me protons of the PF_2Me group develop unequal $^{3}J_{FH}$ coupling constants to the (now nonequivalent) fluorines. The data for IIa are reported in Table III. One of the two values of $^{3}J_{FH}$ for the PF_2Me group at low temperature is close to the value for the $PFMe_2$ group (there is no observable difference in $^{3}J_{FH}$ for these two methyls) and it is therefore assigned as due to the axial fluorine: the values of $^{3}J_{FH}$(ax) and $^{3}J_{FH}$(eq) are markedly different. The larger

TABLE II

Barriers to pseudorotation at coalescence temperatures for II and III

	$\Delta G\ddagger$ (T_c)[a]/ kcal mol^{-1} (kJ mol^{-1})	spectral region used	T_c/K	$\Delta\nu$[b]/Hz
IIa	11.1[c,d] (46)	^{31}P-{^{1}H} (part)	273	[d]
IIa	>19[e,f] (>78)	^{1}H (NMe region)	>353	~10
IIb	7.8[e] (33)	^{19}F-{^{1}H}	188	1520[g]
IIb	14.5[f] (61)	^{1}H (NMe region)	268	3.9[h]
IIIa	22.9[f] (96)	^{1}H (NMe region)	433	11.0[i]
IIIb	15.5[f] (65)	^{1}H (NMe region)	293	8.2[i]

[a] Probably accurate to ±1 kJ mol^{-1} except for IIb (^{1}H measurement) and IIIa where it is ±2 kJ mol^{-1} A transmission coefficient, $\kappa = 1$, has been used in the derivation of $\Delta G\ddagger$.

[b] Used in the coalescence equation $k_r(T_c) = \pi\Delta\nu/\sqrt{2} = (kT_c/h)\exp(-\Delta G\ddagger/RT)$.

[c] Fluorine axial ⇌ equatorial barrier.

[d] Bandshape fitting using the computer programme WAX; this procedure also gave $\Delta H\ddagger = 49 \pm 4$ kJ mol^{-1}, $\Delta S\ddagger = 4 \pm 3$ J mol^{-1}K^{-1}.

[e] For a solution in ortho-dichlorobenzene.

[f] P—N bond equilibration barrier.

[g] ^{19}F chemical shift difference.

[h] ^{1}H chemical shift difference.

[i] L_{PH} for the NMe resonance.

of the two values of $|^3J_{PNCH}|$ for each NMe is tentatively assigned to the equatorial coupling by comparison with data[17] for compound VI. Further evidence that the equatorial value is the larger is provided by the results of The and Cavell[18] for $(CF_3)_3(CH_3)PNMe_2$, where the NMe_2 group is assumed to be equatorial and $|^3J_{PNCH}|$ is 13.3 Hz. Moreover, for $[F_3PNMe]_2$ the value of $|^3J_{PH}|$ from the NMe protons (14.1 Hz) is greater than that for $[MeF_2PNMe]_2$ (12.5 Hz), and the average value for compound IIIa (see below) is even smaller, so we suggest the assignments as in VII.* The low-frequency NMe proton band of IIa shows additional splitting due to (F, H) coupling. The splitting structure corresponds to quartets rather than doublets, implying roughly equal coupling to each fluorine. Previous data[1b,19] on related fluorinated phosphadiazetidinones show (F, H) coupling constants of approximately the same magnitude (1–1.5 Hz) from an axial fluorine to an axial NMe group but not to an equatorial NMe.

*Assignments of $^3J_{PH}$ are not unambiguous; however, as illustrated for the compound $Me_2(Me_2N)P(pfp)$ (pfp = perfluoropinacolyl group); c.f. M. Volkholz, O. Stelzer, and R. Schmutzler, *Chem. Ber.*, **111**, 890 (1978). Assuming that this compound has a structure close to trigonal-bipyramidal, the position of the NMe_2 group is likely to be axial. The observed value of $^3J_{PH}$ (14.5 Hz) is disquietingly high, unless there is a significant departure in stereochemistry from trigonal-bipyramidal.

TABLE III

^{1}H NMR data for the methyl compounds IIa and IIIa

Compound	Temp./°C	δ_H/p.p.m.[a]			$\lvert^2J_{PH}\rvert$/Hz[b]		$\lvert^3J_{FH}\rvert$/Hz[b]		$\lvert^3J_{PH}\rvert$/Hz
		PF_2Me	$PFMe_2$	NMe	PF_2Me	$PFMe_2$	PF_2Me	$PFMe_2$	
IIa	36	1.457	1.382	2.47[c,d]	17.75	14.9 ± 0.1	6.85	10.5 ± 0.1	7.9 ± 0.2[e] 15.9 ± 0.2[e]
				2.45[c,e]					4.8 ± 0.2[e] 17.9 ± 0.2[e]
	−60	1.398	1.332[f] 1.298[f]		17.55	14.5 ± 0.1[g]	10.35(ax) 3.30(eq)	10.7 ± 0.1[g]	
IIIa	36	—	1.437	2.439[h]	—	14.0 ± 0.3 [$^4J_{PH}$ = 0.8 ± 0.3]	—	10.5 ± 0.3 [$^5J_{PH}$ = 0.5 ± 0.3]	16.5 ± 0.3[e] 5.5 ± 0.3[e]

[a] ±0.003 p.p.m. except where otherwise stated.

[b] ±0.05 Hz except where otherwise stated. The sign of $^3J_{PH}$ was found to be positive (assuming $^1J_{PF}$ is negative) by heteronuclear double resonance experiments on compound IIIa.

[c] For a tentative assignment see the text.

[d] The coupling constants to ^{19}F are ≤ 1.2 Hz.

[e] There is a splitting of 1.4 ± 0.1 Hz due to coupling to the fluorines (see the text).

[f] Absolute assignment unknown.

[g] No observable difference between the values for the two methyl groups.

[h] The two values of $\lvert^4J_{FH}\rvert$ are 1.4 Hz and 1.2 Hz, the sum being much more accurately determined than the difference.

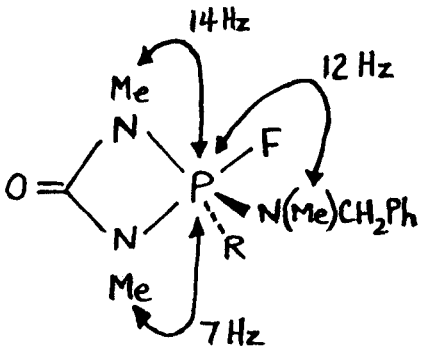

VI (R = Me or Ph)

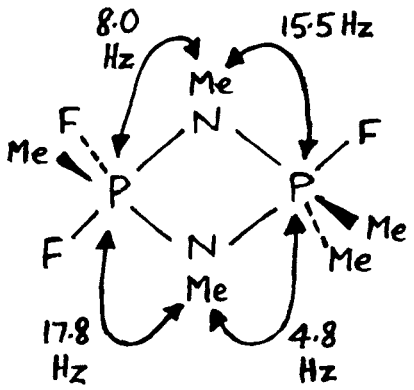

VII

Similar effects occur for the corresponding methoxy compound IIb (see Table IV) but since P—N bond equilibration is faster than in the case of IIa, the NMe region is essentially a triplet (with a small splitting of the central peak) at ambient probe temperature, becoming a pair of double doublets (with some further splitting and broadening due to (F, H) coupling, as for compound IIa) at −40°C, as P—N equilibration is slowed. The coalescence temperature (ca. −5°C) yields the barrier information given in Table II. Assignment considerations for the coupling constants parallel those for compound IIa, but since the average value of $^3J_{PH}$ is very similar for the two NMe groups it is not possible to assign the two chemical shifts. The OMe region of the ^1H spectrum for IIb is second order (since the ^{31}P nuclei are strongly coupled) and has not been fully analysed. However, ^1H-{^{19}F} double resonance experiments enabled values of δ_H and N_{PH} to be obtained, and these are given in Table IV.

Proton spectra of the difluorodiazadiphosphetidines (III)

It has been shown earlier[8] that P—N bond equilibration is slow for $[Ph_2FPNMe]_2$ on the NMR timescale at ambient probe temperature, and that the NMe proton spectrum could therefore be explained on the basis on an $[AMX_3]_2$ spin system (ignoring the phenyl protons). The ambient-temperature ^1H spectrum (NMe region) of IIIa is virtually identical to that of $[Ph_2FPNMe]_2$ and the data are given in Table III. As the temperature is raised, however, the central lines of the spectrum coalesce (at ca. 433K) as the effective spin system (excluding the PMe protons) tends to become $[AM]_2X_6$. At 333K the NMe proton spectrum of IIIb (see Table IV) is already a triplet with fine splittings due to (F, H) coupling (Figure 5A), and cooling is necessary to slow P—N bond equilibration (Figure 5B). At ambient probe temperature the spectrum is in an intermediate state. The low-temperature NMe spectrum may also be explained on an $[AMX_3]_2$ basis but the $[ph_3]_2$ subspectrum (see Ref. 8) is deceptively simple due to the large value of $|J_{PP}|$. The clearest change with temperature for both IIIa and IIIb is the collapse of the intense lines separated by $L_{PH} = |^3J_{PH} - {}^3J'_{PH}|$. This change may be used to determine barriers to P—N equilibration from coalescence temperatures (detailed bandshape fitting is not feasible because of the complex nature of the exchanging spin systems). The barrier information is given in Table 2. For both IIIa and IIIb the larger of the two values of $^3J_{PH}$ is tentatively assigned to the equatorial pathway, as for IIa and IIb (see above).

TABLE IV

^{1}H data[a] for the methoxy compounds IIb and IIIb

Compound	Temp./°C	Methoxy region δ_{OMe}/p.p.m.	Methoxy region $\lvert^3J_{PH} + {}^5J_{PH}\rvert$/Hz	Methoxy region $\lvert^4J_{FH} + {}^6J_{FH}\rvert$/Hz	NMe region δ_{NMe}/p.p.m.	NMe region $\lvert^3J_{PH}\rvert$/Hz	NMe region $\lvert^4J_{FH}\rvert$/Hz
IIb	35	3.642 ($OMe)_2$ 3.647 (OMe)	14.3 14.5	[b]	2.420	12.0[c] 12.5[c]	~0.5
	−40	[b]	[b]	[b]	2.466[c]	9.1[c] 15.8[c]	<1.0
					2.427[c]	7.7[c] 17.0[c]	<1.5
IIIb	65	[b]	[b]	[b]	2.361	12.3	0.5
	−45	3.587	13.75 ± 0.05	1.75 ± 0.05	2.361	16.3[c] 8.1[c]	0.45 0.55

[a] Chemical shifts are accurate to ±0.003 coupling constants to ±0.2.
[b] Not obtained.
[c] Absolute assignment unknown (see the text), but the larger values of $\lvert^3J_{PH}\rvert$ are tentatively assigned as due to the equatorial pathways.

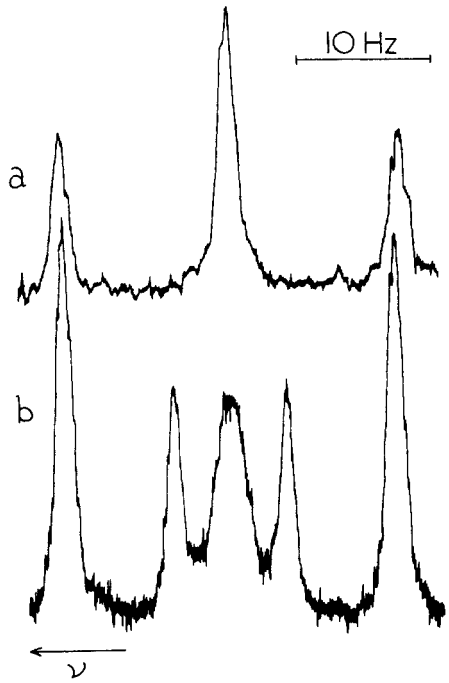

FIGURE 5 ^{1}H spectra (NMe region) for $[(MeO)_2FPNMe]_2$. (a) +60°C; (b) −30°C.

The PMe_2 region of the proton spectrum of IIIa is complex at room temperature. In principle, ignoring the NMe protons, it is of the $[AMX_6]_2$ type, and calculations on this basis allowed us to obtain the data of Table III, some discrepancies between the experimental and calculated spectra being attributed to the effects of the NMe protons. The $P(OMe)_2$ region of the proton spectrum of IIIb looked simpler, mainly because of conditions approaching deceptive simplicity. Only values of δ_H, N_{PH} and N_{FH} were obtained in this case; these results are given in Table 4.

Proton spectral analysis for compounds IIIa and IIIb was assisted by ^{1}H-{^{19}F}decoupling experiments.

Intermolecular mechanisms of fluorine exchange

It has been demonstrated[20,21] that the rate of fluorine exchange in Me_2NSF_3 and Et_2NSF_3 is greatly accelerated by the presence of trace amounts of water or HF. However, the exchange rate may be reduced by the addition of silicon-nitrogen compounds such as Me_3SiNR_2 or $(Me_3Si)_2NH$ which reduce the concentration of H_2O and HF by chemical reaction. In the above cases the hydrolysis provides the lowest energy pathway for fluorine exchange. The mechanism of this exchange is envisaged to be a Lewis acid-Lewis base interaction and rapid equilibration of five- and six-coordinate geometries. Moreover, PF_5 is known to form 1:1 complexes with a variety of Lewis bases, and the structure of such a complex is shown to be octahedral on the basis of the fine structure observed in the ^{19}F spectrum:[22]

$$PF_5 + \text{base} \rightleftharpoons PF_5\text{:base}$$

In view of the above observations it was considered important to investigate the possibility of intermolecular fluorine exchange in diazadiphosphetidines by the presence of trace amounts of water. Spectra were recorded before and after the addition of a few drops of $(Me_3Si)_2NMe$ (scavenger). There was no appreciable change for penta-, tetra- and tri-fluorodiazadiphosphetidines, on the addition of the scavenger. However, for an old sample of IIIa the addition of a few drops of $(Me_3Si)_2NMe$ produced a narrowing of lines in the ^{19}F and ^{1}H spectra. It is the triplets due to (H, F) coupling that become broad in the old sample; this shows some sort of fluorine exchange in this compound. The analogous compound, IIIb, does not show any change in the presence of traces of water. The compounds of the type $[R_2FPNMe]_2$ where R = alkyl or phenyl were thought[23] to be difficult to make, on account of their instability. Perhaps the observations on which this conclusion was based are actually due to the fact that these compounds are prone to intermolecular fluorine exchange by traces of water. The barrier determination for $[Me_2FPNMe]_2$ reported here was carried out in the presence of a few drops of $(Me_3Si)_2NMe$.

DISCUSSION

For diazadiphosphetidines there are 18 feasible pseudorotamers[10] (excluding mirror images) such that each ring-nitrogen is axial to one phosphorus and equatorial to the other. Such structures can be conveniently represented by projections on to a plane perpendicular to the P—P direction, as in Figure 6. In these projections the broken double line indicates the plane of the $(PN)_2$ ring, and the two substituents along this line are axial to a phosphorus, while the other four are equatorial. We assume that the stable pseudorotamers of the compounds studied here have only fluorine atoms at exocyclic axial positions (this is confirmed by the axial NMR character of the PFR_2 fluorine for II and III at all temperatures studied). There are 8, 4 and 2 of such forms (excluding mirror images) for compounds of types I, II and III respectively, and these are illustrated in Figure 6. For the tetrafluoro-diazadiphosphetidines four of the forms have a *gauche* arrangement of the substituents R, and four have *trans* substituent relationships. We have information on the rates of five pseudorotation processes in these compounds, viz:

(i) axial $\rightleftharpoons$ equatorial fluorine exchange for $[RF_2PNMe]_2$(I)
(ii) *Gauche* $\rightleftharpoons$ *trans* exchange for $[RF_2PNMe]_2$(I)
(iii) Axial $\rightleftharpoons$ equatorial fluorine exchange for $R^1F_2P(NMe)_2PFR^1_2$(II)
(iv) P—N bond equilibration for $R^1F_2P(NMe)_2PFR^1_2$(II)
(v) P—N bond equilibration for $[R^2_2FPNMe]_2$(III).

The most rapid of these five processes for a given substituent $R = R^1 = R^2$ is the first—indeed, we have not succeeded in obtaining a low enough temperature to stop this exchange on the NMR timescale for any compound. The results given here show that, in the rather limited number of cases studied, processes (ii) and (iii) have comparable barriers, as have processes (iv) and (v), but the latter barriers are about twice the former. Figure 7 summarises the situation. There is a similar situation, including the rapidity of a process analogous to (i), for fluorinated phosphadiazetidinones of the types VIII, IX and X.

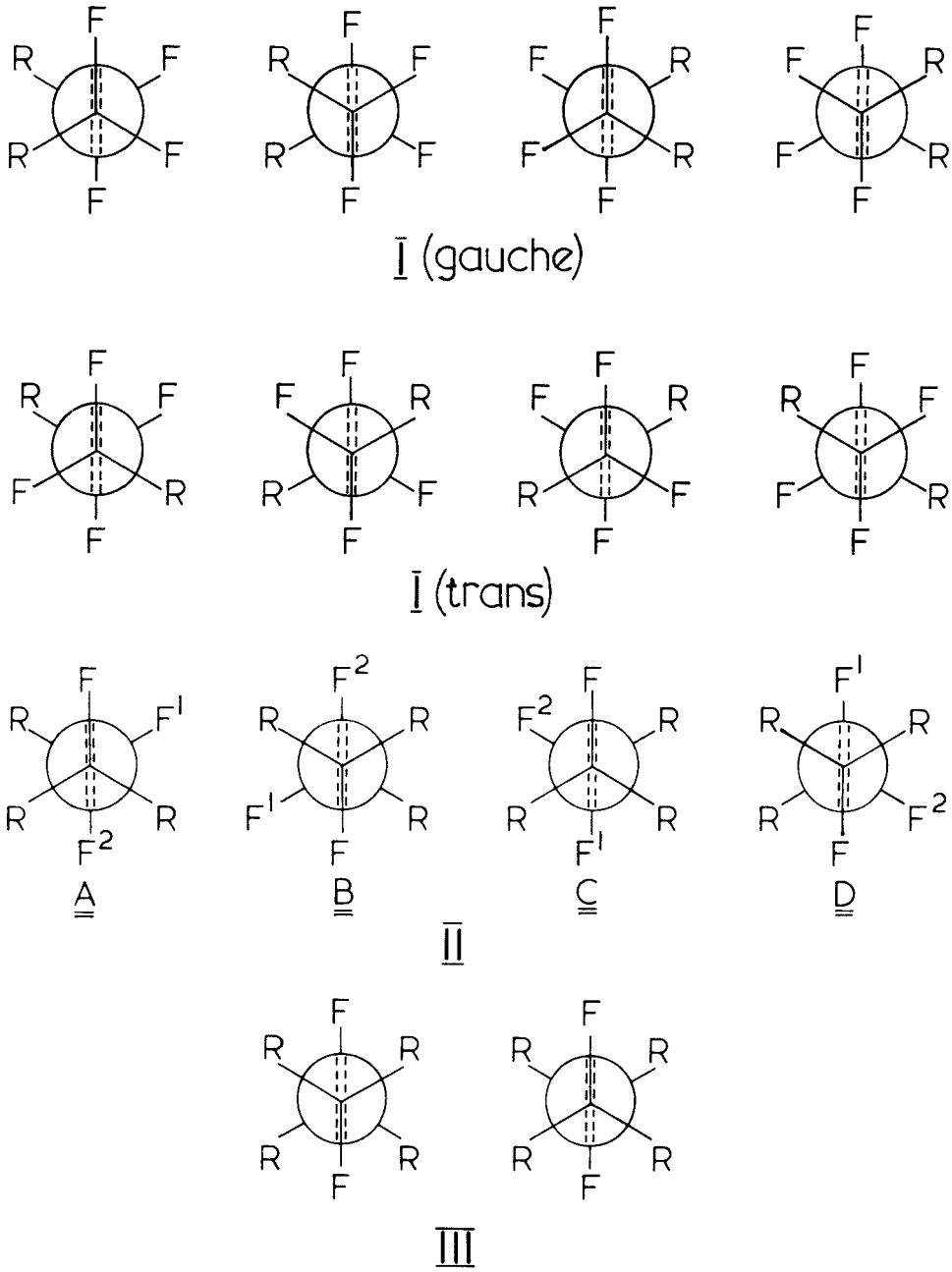

FIGURE 6 The conformers of compounds I, II and III which are assumed to be the stable ones. The dashed line indicates the plane of the P_2N_2 ring.

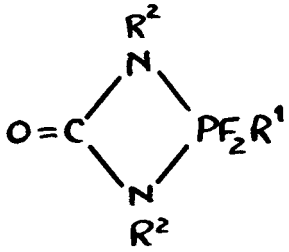

VIII

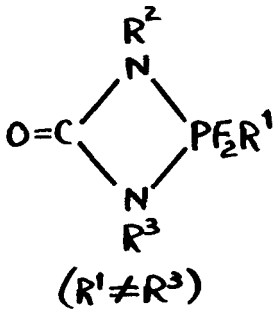

IX

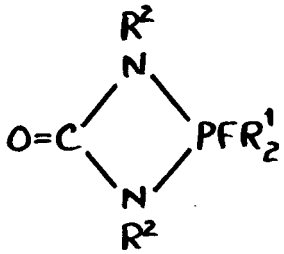

X

Moreover, the magnitude of the barrier for rendering the fluorine nuclei equivalent in IX, $R^1 = R^2 = Me$, $R^3 = Et$, is comparable to that for processes (ii) (I, R = Me) and (iii) (II, R^1 = Me). However, for diazadiphosphetidines of type II, the relative rigidity of the PFR_2 group effectively prevents the fastest of the processes occurring at the PF_2R moiety.

These facts can be rationalised if it is assumed, firstly that pseudorotation at the two phosphorus atoms in diazadiphosphetidines occurs essentially independently (at least in compounds of the type II), and secondly that the barrier to 180° pseudorotation of a PFR_2 group (which involves two intermediates with an axial R group) is roughly twice as big as that to 120° pseudorotation of a PF_2R group (which involves one such intermediate). Actually, the latter condition implies the former.

In an earlier publication,[10] we suggested that pseudorotation in tetrafluorodiazadiphosphetidines (I) was concerted at the two phosphorus atoms, rather than independent, partly because, strictly speaking, the latter procedure would produce an intermediate with one ring-nitrogen axial to both phosphorus and the other equatorial to both (a situation which would involve ring-strain). The evidence for I and for III is consistent with concerted pseudorotation behaviour, *with the added assumption that the barrier depends on the number of R groups in axial positions in the highest-energy metastable intermediate*, but the situation for the trifluorodiazadiphosphetidines (II) cannot be readily reconciled with such a hypothesis.* For these compounds (II), as explained above, there are two observable physical processes, viz. axial$\rightleftharpoons$equatorial exchange of F^1 and F^2 (with concomitant exchange of R-group environments for the PFR_2 moiety), and P—N bond equilibration. The equivalent exchanges A$\rightleftharpoons$D and B$\rightleftharpoons$C (see Figure 6) accomplish both P—F and P—N bond equilibration. However, A$\rightleftharpoons$C and B$\rightleftharpoons$D exchanges equilibrate only the P—F bonds, whereas A$\rightleftharpoons$B and C$\rightleftharpoons$D equilibrate only the P—N bonds. Our

* Reference 12 contains a misprint on page 1919 which incorrectly implies that conformational exchange in compounds of type II *must* occur by pseudorotation at one phosphorus alone. The intended statement in that paper merely emphasized that both concerted pseudorotation and independent pseudorotation can only occur via forms with axial substituents other than fluorine.

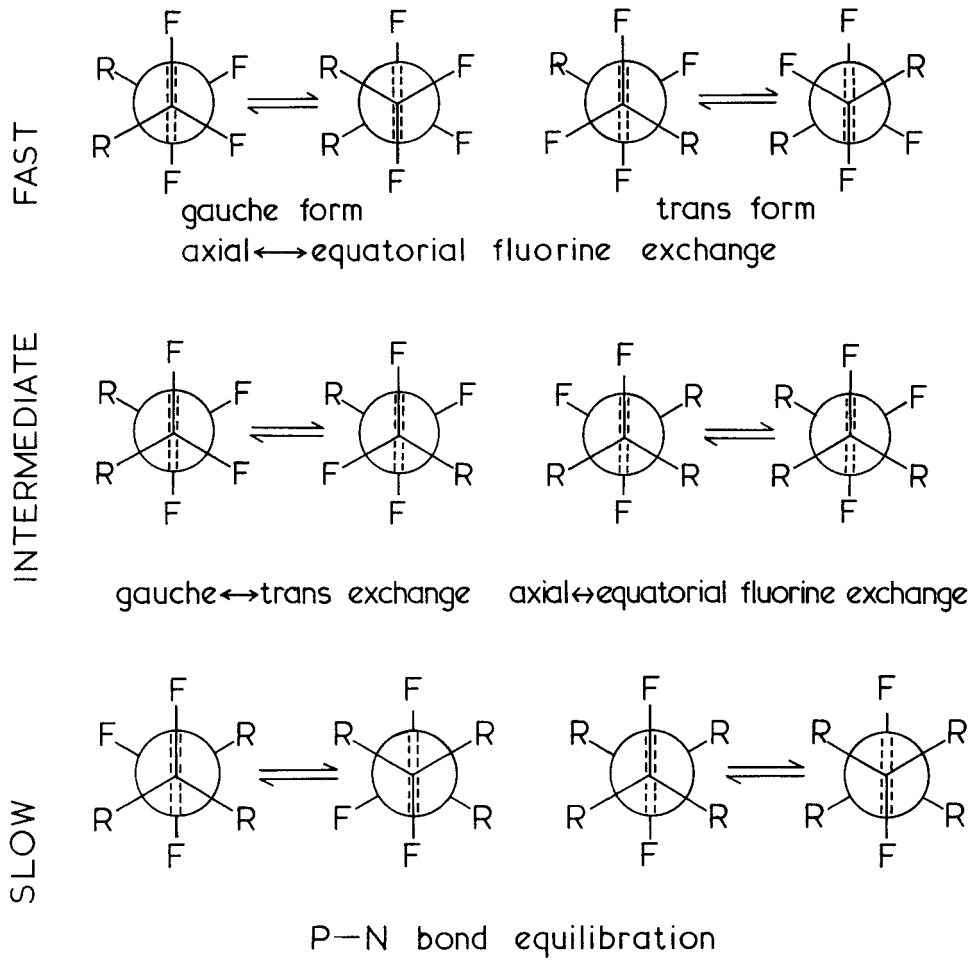

FIGURE 7 Summary of the exchange rate information obtained for compounds I, II and III. The dashed line indicates the plane of the P_2N_2 ring.

observation that P—F bond equilibration has a barrier only ca. one-half that of P—N bond equilibration shows that the A⇌C, B⇌D process (for which the PFR_2 group remains unchanged) is the dominant one, which can only be the case if the PF_2R group pseudorotates essentially independently of and much faster than the PFR_2 moiety. However, doubtless there will be some degree of adjustment at the second phosphorus when one pseudorotates, so as to minimise the energy of the activated state (the barrier). Indeed, this adjustment could occur after the fashion of Figure 8, which avoids any intermediate with one ring-nitrogen axial to both P atoms, and which essentially describes a concerted process. It is therefore the assumption that the barrier is determined by the number of R groups axial in an intermediate which has to be abandoned in favour of the hypothesis that the barrier to pseudorotation of a PFR_2 group alone is roughly twice that of a PF_2R group (see

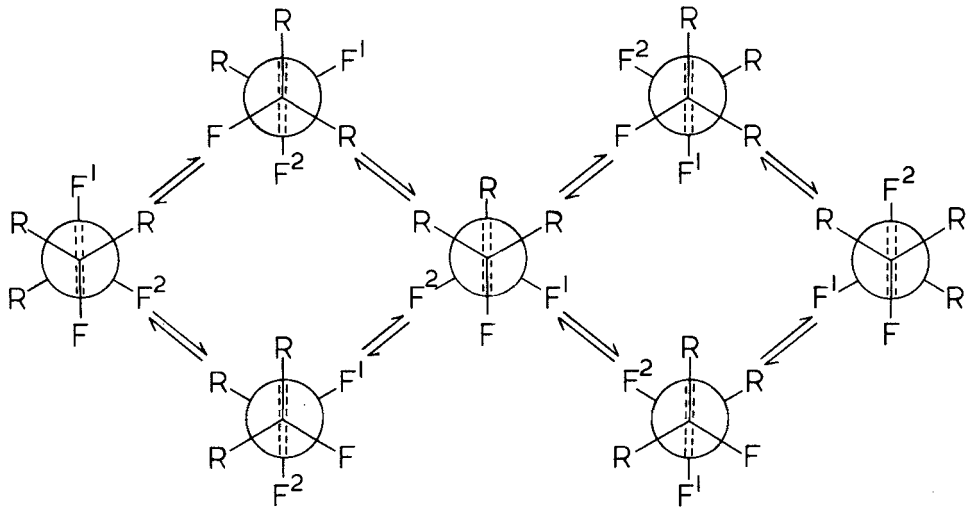

FIGURE 8 A possible concerted pseudorotation pathway for axial⇌equatorial fluorine exchange in trifluorodiazadiphosphetidines which would *not* lead to P—N bond equilibration. The dashed line indicates the plane of the P_2N_2 ring.

also Ref. 1b). The former assumption leads to roughly equal rates of II A⇌B, A⇌C and A⇌D (and therefore to roughly equal rates of P—N and P—F bond equilibration) since in all cases only intermediates with one R group axial need be involved in a concerted process.

The activation parameters for *trans*⇌*gauche* interconversion in $[RF_2PNMe]_2$ are given in the Table I. $\Delta H\ddagger$ and $\Delta S\ddagger$ are those obtained from the least-squares fits of the data. Actual errors in these parameters are large; about 25–50% in the case of $\Delta S\ddagger$. For instance, it is found that the scatter of points was such that it is possible to get equal $\Delta S\ddagger$ values for both Ia and Ib. The results for Ie are considered to be the least accurate (the large negative $\Delta S\ddagger$ is almost certainly unrealistic) because of the poor signal-to-noise ratio of the spectra. In the Eyring plotting procedure a transmission coefficient, κ, of 1 has been used. Negative values of $\Delta S\ddagger$ can arise, for several reasons, among them being the existence of metastable intermediates such as may occur in the present cases. It is well-known that NMR bandshape fitting frequently gives mutually-compensating systematic errors in $\Delta H\ddagger$ and $\Delta S\ddagger$. For this reason we shall not discuss such data further, though it is encouraging to note that there are clear trends in these parameters with substituent bulk. However, the bandshape fitting is viewed as a method of getting rather accurate values (probably to within ± 1 kJ mol^{-1}) for $\Delta G\ddagger$ in the vicinity of T_c, so it is these results which will be used to compare the barriers to exchange.

For compounds of type I the concerted pseudorotation pathway of Figure 13 of Ref. 10 may still apply (particularly for axial⇌equatorial fluorine exchange), though it should be stressed that it is not really known whether any intermediate structures depicted represent potential minima (i.e. are genuine intermediates) or maxima in the exchange process, or whether they are not on the minimum-barrier exchange profile at all. However, it is likely that forms in which one R group is

axial *are* metastable intermediates in the *gauche* $\rightleftharpoons$ *trans* exchange process, in which case the barrier should depend on the apicophilicity of R, which in turn will be effected by the electronic and steric properties of R.

For the alkyl series the barrier increases in the order Me < Et < Pr^i < Bu^t. Since the electronegativity effects are very similar for these groups the differences in the barrier heights must be attributed to differences in their steric effects. Long-range steric effects are not easy to visualise in terms of molecular models; the various groups do not appear to interfere with one another significantly. Perhaps the effect is the steric hindrance to solvation, or involves bond-angle changes consequent upon interactions at each phosphorus separately. The barrier for the phenyl compound, Ie, is similar to that of the ethyl compound, Ib. This is not surprising in view of the planar structure of the phenyl group, with minimum steric requirements and slightly larger electronegativity.

We have studied (in less detail) several other compounds of type I in order to obtain information on the effect of substituent electronegativity on *gauche* $\rightleftharpoons$ *trans* exchange. We find that such electronegativity effects are very important in deciding the barrier to pseudorotation. Thus, it did not prove possible to slow the *gauche* $\rightleftharpoons$ *trans* process for the compound $[MeOF_2PNMe]_2$. No broadening of the spectrum was observed even at the lowest temperature feasible (−120°C, for a solution in vinyl chloride). This is presumably due to the increased electronegativity of the methoxy group, which makes it easier to occupy an axial site, i.e. increases its apicophilicity. For $[NEt_2F_2PNMe]_2$ broadening of the spectrum starts around −100°C and coalescence was observed around −117°C. However, it was not possible to observe separate resonances for *trans* and *gauche* isomers. Even though NEt_2 is a fairly bulky group, the low barrier (~29 kJ mol^{-1}, assuming a chemical shift of 200 Hz and equal populations) can be attributed to the increased electronegativity of the NEt group reducing its aversion to occupying an axial site.

It is interesting to compare the *gauche* $\rightleftharpoons$ *trans* exchange barriers for the compounds I where R = Pr^i and Bu^t with those for R = $CHCl_2$ and CCl_3, since the steric effects of Me and Cl groups are similar. Exchange barriers for the latter pair of compounds were obtained using coalescence[24] of the unequally populated[13] N-doublet lines. Values of $\Delta G\ddagger$ for R = $CHCl_2$ and CCl_3 are similar and are of the order of 52 kJ mol^{-1}, compared to (Table 1) 68 kJ mol^{-1} for R = Pr^i and 82 kJ mol^{-1} for R = Bu^t. The lower barriers for the chloromethyl compounds are attributed to the higher electronegativity of the groups. In going from —$CHCl_2$ to —CCl_3 the barrier seems to be relatively unchanged, presumably due to the higher electronegativity of the CCl_3 group offsetting the increased steric effect.

Attempts to slow the axial $\rightleftharpoons$ equatorial exchange of fluorine in the two isomers of Id failed. No broadening of the resonances of the two isomers was observed down to −100°C but the low-frequency isomer (*trans*) showed slight broadening at −125°C. The low-frequency isomer of Ib showed rapid broadening at low tempertures and coalescence at −100°C. However, the slow-exchange limit spectrum could not be obtained because of the unattainability of appreciably lower temperatures. The barrier to axial $\rightleftharpoons$ equatorial fluorine exchange in this compound should be around 25–29 kJ mol^{-1} (assuming the value for the axial-equatorial fluorine chemical shift difference found for IIa at low temperatures). The apparently higher barrier for axial $\rightleftharpoons$ equatorial exchange for the *trans* isomer than for the *gauche* isomer is at first sight surprising, since for the *gauche* isomer the two R groups must pass each other, whereas in the *trans* isomer the R groups are far apart. On the other

hand, the chemical shift difference for the fluorines at the two sites in the *trans* isomer may be larger than in the *gauche* isomer, and, as already stated, molecular models do not suggest much long-range steric hindrance. The fractional population of the *gauche* form decreases in the order Me > Et ~ Ph > Pr^i > Bu^t, as shown by the $\Delta G^{\ominus}$ values (see Table I). For Ia the *trans* and *gauche* populations are nearly equal, but as the bulk of the R group increases the *trans* isomer becomes more favoured. (In fact the assignment of the high- and low-frequency isomers to *gauche* and *trans* forms, respectively, was made on this basis and must be regarded as only tentative). However, molecular models show very little or no steric hindrance between the two R groups in the *gauche* isomer. This trend, where the relative population of *gauche* to *trans* decreases with substituent size, is also observed for the series Me > CH_2Cl > $CHCl_2$ > CCl_3, showing that this is entirely due to steric effects and not to any electronic effects.

The discussion earlier in this section suffices to explain why the barriers to P—F and P—N bond equilibration in compounds of the type II are different. Because these two equilibrations involve pseudorotation at the PF_2R and PFR_2 groups respectively, the barriers are similar to those for *gauche* $\rightleftharpoons$ *trans* exchange in I and P—N bond equilibration in III, respectively. The pseudorotation process for P—F bond equilibration in II must involve an R group passing the $(PN)_2$ plane, i.e. becoming axial, thus raising the barrier above that for the axial $\rightleftharpoons$ equatorial fluorine exchange in I. The low barrier to axial $\rightleftharpoons$ equatorial exchange in IIb again shows that more electronegative substituents are less reluctant to occupy axial sites. On the basis of the results for IIb it is surprising that *trans* $\rightleftharpoons$ *gauche* exchange in $[(OMe)F_2PNMe]_2$ could not be slowed even at −125°C. This is perhaps due to the chemical shift difference between the two isomers being small.

The barrier to P—N equilibration for compound IIIb is comparable to that in IIb because both involve a 180° pseudorotation of a PFR_2 group, which is known[1b] to be difficult in the phosphadiazetidinone series. Whether the process for III passes through an intermediate such as XI (which has two R groups axial and implies concerted pseudorotation) or such as XII (which has one R group axial, plus a strained ring, and implies independent pseudorotation) is not known. In either case one would have expected a larger barrier than that to P—N equilibration in the corresponding compound II. Apparently the dominant factor is simply the rigidity of the PFR_2 group, in contrast to the PF_2R group. Once again, the substituent electronegativity is very important, since the barrier for IIIb is substantially less than that for IIIa.

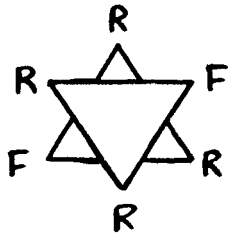

XIa

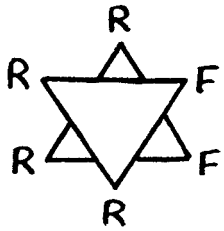

XIb

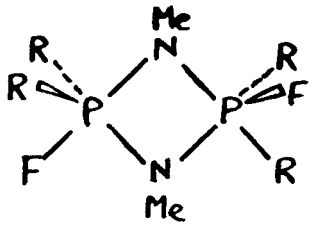

XII

EXPERIMENTAL

The ^{19}F-{^1H} NMR experiments were carried out at 94.155 MHz using a Varian HA100 spectrometer in the frequency-sweep mode, in conjunction with a Schlumberger FSX 3005 frequency synthesizer (provid-

ing the 100 MHz ^1H irradiation), a Hewlett-Packard 3722A noise generator and a double-tuned probe as described previously.[12] The $^{31}P-\{^1H\}$ spectra were obtained at 40.5 MHz using a Varian XL-100 NMR spectrometer in the CW mode. Multiscan averaging of the ^{31}P spectra was carried out by interfacing a Varian 620/i computer to the spectrometer. Proton NMR spectra were obtained using the Varian HA100 spectrometer operating at 99.896 MHz. The reported proton shifts were measured directly with respect to internal TMS, and higher chemical shifts imply higher frequencies.

Spectra at room temperature and below were recorded using solutions made up in a 1:1 CD_2Cl_2 and CH_2Cl_2 solvent mixture, plus a few drops of $CFCl_3$ to provide a field-frequency lock for ^{19}F resonance. The CD_2Cl_2 provided the ^2H lock signal for the XL-100 work and Me_4Si was added to serve the same purpose for the HA 100 ^1H studies. The sample tubes were of 5 mm outside diameter; samples were degassed and sealed. Spectra below −100°C were obtained for samples dissolved in vinyl chloride, using a special probe.[25] Spectra above room temperature were obtained in samples dissolved in 1,2,4-trichlorobenzene as solvent (except for the ^1H study of compound IIa, for which ortho-dichlorobenzene was used). For the ^{19}F bandshape studies the temperature was calibrated using[26] the ^{19}F chemical shift difference in a sample of 10% $(CFCl_2)_2$, 10% $(CF_2Br)_2$ and 80% butylbenzene.

ACKNOWLEDGEMENTS

We thank N. Weferling for the preparation of a sample of compound IIa. We acknowledge support from Fonds der Chemischen Industrie, Deutsche Forschungsgemeinschaft and Bayer AG.

REFERENCES

1. (a) Part 1: S. C. Peake, M. J. C. Hewson, O. Schlak, R. Schmutzler, R. K. Harris and M. I. M. Wazeer, *Phosphorus and Sulfur*, **4,** 67 (1978).
   (b) Part 2: O. Schlak, R. Schmutzler, R. K. Harris, E. M. McVicker and M. I. M. Wazeer, *Phosphorus and Sulfur*, in press.
2. A. Almenningen, B. Anderson and E. E. Astrup, *Acta Chem. Scand.*; **23,** 2179 (1969).
3. H. Hess and D. Forst, *Z. anorg. allg. Chem.*, **342,** 240 (1966).
4. L. G. Hoard and R. A. Jacobson, *J. Chem. Soc.*, (A) 1203 (1966).
5. J. W. Cox and E. R. Corey, *Chem. Comm.*, 123 (1967).
6. M. Fild, W. S. Sheldrick and T. Stankiewicz, *Z. anorg. allgem. Chem.*, **415,** 43 (1975).
7. W. S. Sheldrick and M. J. C. Hewson, *Acta Cryst.*, **B31,** 1209 (1975).
8. R. K. Harris, M. I. M. Wazeer, O. Schlak, R. Schmutzler and W. S. Sheldrick, *J. C. S. Dalton*, 517 (1977).
9. R. K. Harris and C. M. Woodman, *Mol. Phys.*, **10,** 437 (1966).
10. R. K. Harris, J. R. Woplin, R. E. Dunmur, M. Murray and R. Schmutzler, *Ber. Bunsenges. Phys. Chem.*, **76,** 44 (1972).
11. O. Schlak, R. Schmutzler, R. K. Harris and M. Murray, *J. C. S. Chem. Comm.* 23 (1973).
12. R. K. Harris, M. I. M. Wazeer, O. Schlak and R. Schmutzler, *J. C. S. Dalton*, 1912 (1974).
13. R. K. Harris, M. Lewellyn, M. I. M. Wazeer, J. R. Woplin, R. E. Dunmur, M. J. C Hewson and R. Schmutzler, *J. C. S. Dalton*, 61 (1975).
14. R. K. Harris, M. I. M. Wazeer, O. Schlak and R. Schmutzler, *J. C. S. Dalton*, 17 (1976).
15. E. L. Hahn and D. E. Maxwell, *Phys. Rev.*, **88,** 1070 (1952).
16. H. M. McConnell, *J. Chem. Phys.*, **28,** 430 (1958).
17. O. Schlak, Diplomarbeit, Technische Universität Braunschweig, 1971.
18. K. I. The and R. G. Cavell, *Inorg. Chem.*, **16,** 2887 (1977).
19. R. K. Harris and C. J. Macdonald, unpublished work.
20. A. F. Janzen, J. A. Gibson and D. G. Ibott, *Inorg. Chem.*, **11,** 2853 (1972).
21. D. G. Ibott and A. F. Janzen, *Canad. J. Chem.*, **50,** 2428 (1972).
22. J. A. Gibson, D. G. Ibott and A. F. Janzen, *Canad. J. Chem.*, **51,** 3203 (1973).
23. R. Schmutzler, *J. C. S. Dalton*, 2687 (1973).
24. H. Shanan-Atidi and K. H. Bar-Eli, *J. Phys. Chem.*, **74,** 961 (1970).
25. A. Sinclair, Ph.D. thesis, University of East Anglia, 1972.
26. V. J. Gazzard and N. C. Pyper, unpublished work.